Chemical Physics Impact 6 (2023) 100140

Contents lists available at ScienceDirect

Chemical Physics Impact

journal homepage: www.sciencedirect.com/journal/chemical-physics-impact

Solvent effects on glyphosate deprotonation: DFT theoretical studies

Alberto G. Albesa *, María Estefanía Farías Hermosilla

INIFTA (Depto. de Química, Fac. Cs. Exactas, UNLP, CONICET) Casilla de Correo 16, Sucursal 4, (B1904DPI), La Plata, RA, Argentina

ARTICLE INFO

Keywords:
Glyphosate
DFT calculations
Conformes
Solvent effects
NMR

ABSTRACT

To better understand the molecular structures of glyphosate in different solvents, we have studied several possible conformations, and their relative abundances, of glyphosate and its deprotonated forms, in acetone, acetonitrile, DMSO, water, ethanol, carbon tetrachloride, dichloromethane and gas phase. We have also studied NMR and IR spectra of these species in these solvents. We found that the first protonation of glyphosate in water corresponds to the protonation on the amino group, the second protonation in the phosphonate group, the third protonation in the carboxylic group, and that when the molecule has a neutral charge, the most stable form is the zwitterionic specie with the protonated amino group and the phosphonate group.

1. Introduction

Pesticides are defined by the FAO/WHO as substances (or mixtures of substances) that are used to prevent or control undesirable animals or plants.

In regions that have a high consumption of pesticides, it is common to observe their presence in groundwater and aquifers [1].

Herbicides have been found to be most responsible for water pollution [2]. This is due to: a) they are the most widely used pesticides, b) they have greater solubility in water and are less retained in organic carbon than the rest of the pesticides, c) they are applied directly to the soil, and d) they have a high persistence in soil.

Having the ability to detect this type of substance is essential for economic and social development, taking into account the serious consequences of water pollution.

Among them, glyphosate has become the most popular herbicide in the world. The detection and quantification of glyphosate is expensive and slow, and therefore any government measure becomes ineffective since the real impact of its application is unknown. This means that, despite being the most widely used agrochemical in the world, it is the most difficult to determine by analytical means. Glyphosate has ionic character, high polarity and, therefore, high solubility in water, evaporates with difficulty, has low solubility in organic solvents, and forms complexes easily. This is why that the use of a simple analytical method becomes a challenge [3].

Currently there are several methods to detect the presence of this herbicide in water, among which we can mention:

Chromatography techniques: can be used to separate mixtures into their components allowing each part to be analyzed separately. Many approaches to detect glyphosate (GLY) residues use liquid chromatography (LC) [4] or high-performance liquid chromatography (HPLC) [5], gas chromatography (GC) [6], and ion chromatography (IC) [7]. Alternatively, eluates from chromatographic columns can be fed to mass spectrometer (MS) detectors (LC/MS) [8].

Spectroscopic methods: among these we can find: absorption and emission methods [9,10]; enhanced Raman scattering on the surface [11]; surface plasmon resonance [12]; nuclear magnetic resonance [13]. Electrochemical sensors: amperometric and voltammetric methods [14,15]; capillary electrophoresis [16]

Glyphosate removal methods currently include chemical precipitation [16], advanced oxidation [17,18], membrane filtration [19], biodegradation [10], and physical adsorption [20–26].

Knowing the behavior of glyphosate in different solvents is important to be able to design new removal techniques and new detection methods. In this sense, recent works have been dedicated to the structure and conformational properties of glyphosate, either isolated or in solution, however they only focused on using water as a solvent [27–29]. Glyphosate was investigated in this work by initially studying all the structures and possible conformations that corresponded to the neutral and various deprotonated forms of glyphosate that are expected to be found in aqueous solution. The most abundant species were identified and the spectroscopic properties of these species were calculated.

We found that the first protonation of glyphosate in water corresponds to the protonation on the amino group, the second protonation in the phosphonate group, the third protonation in the carboxylic group,

* Corresponding author.
E-mail address: albesa@inifta.unlp.edu.ar (A.G. Albesa).

https://doi.org/10.1016/j.chphi.2022.100140
Received 12 October 2022; Received in revised form 28 November 2022; Accepted 5 December 2022
Available online 6 December 2022

Table 1
Name and number of the conformations considered for each structure investigated in the glyphosate deprotonation reactions.

formal charge (FC)	tautomer structure	name (number)
0	$H_2PO_3CH_2NHCH_2COOH$	4112(5)
GLY	$H_2PO_3CH_2NH_2^+CH_2COO^-$	4202(2)
	$HPO_3CH_2NH_2^+CH_2COOH$	4211(4)
-1	$H_2PO_3CH_2NHCH_2COO^-$	4102(5)
GLY^-	$HPO_3^-CH_2NHCH_2COOH$	4111(3)
	$HPO_3^-CH_2NH_2^+CH_2COO^-$	4201(5)
-2	$HPO_3^{-2}CH_2NHCH_2COO^-$	4101(5)
GLY^{2-}	$PO_3^{-2}CH_2NH_2^+CH_2COO^-$	4200(6)
-3	$PO_3^{-2}CH_2NHCH_2COO^-$	4100(5)
GLY^{3-}		

Table 2
Solvents and dielectric constant.

Solvent	epsilon
Acetone CH_3COCH_3	20.7
Acetonitrile (CH_3CN)	37.5
CH_2Cl_2	10.36
CCl_4	2.24
DMSO	46.7
Ethanol (EtOH)	24.5
water (H_2O)	78.2
Gas phase	1

and that when the molecule has a neutral charge, the most stable form is the zwitterionic specie with the protonated amino group and the phosphonate group.

2. Methodology

The molecules under study were subjected to geometry optimizations using density functional theory [30,31]. For this, we used the hybrid exchange correlation functional B3LYP and the Gaussian basis set functions 6-31G(d,p) and 6–311++G(2d,2p), as implemented in the ORCA package [32]. All geometrical parameters were optimized without constraints.

We used two implicit solvent models to evaluate the solvent effect: the integral equation formalism polarizable continuum model (IEFPCM), [33] and the density-based solvation model (SMD) [34]. Both models consider that the solvent is a continuous medium with a certain dielectric constant. The dielectric constants of the solvents are listed in Table 2. To simulate the effects of exposure of the solute to the solvent, a cavity is opened to place the molecule that is being studied. The cavities have a surface charge that stabilizes according to the dielectric constant of the solvent. The differences between IEFPCM and SMD lie in the definition of the molecular cavity and in their formulation of the terms of the non-electrostatic contributions.

We also performed frequency calculations in all cases, that is, for the gas phase and for the solvated systems, to obtain the corresponding Gibbs free energy standard values (G*298.15K) and the corresponding Boltzmann population values. The importance of the vibrational analysis is two-fold. First, it allows to characterize a given conformation as a true minimum on the molecular potential energy surface, and, if the conformation is confirmed to be a minimum, the calculated harmonic frequencies are useful in the assignment of the experimental vibrational data.

Taking into account that the results of the B3LYP/6-311++G(2d,2p) method in an aqueous medium coincide with the results obtained by Ruano et al., this level of theory is the one that was used to assign the vibrational frequencies.

Finally, we calculated the isotropic chemical shifts for phosphorus atoms. In this case, the isotropic magnetic shielding tensor was obtained at the B3LYP/6-311++G(2d,2p) level of theory. The reported shifts are relative to phosphoric acid. The absolute isotropic shieldings of phosphoric acid were also calculated using the B3LYP/6-311++G(2d,2p) model.

We took the initial conformations each different species with different formal charges from the work of Peixoto et al. [29]. A four-digit number was assigned to label the tautomers with each digit referring to the number of hydrogen atoms present in the alyphatic carbons, amino, carboxylate, and phosphonate groups, respectively, for the species with a given formal charge as presented in Table 1. The number of the conformers for each tautomer specie is also given. The schemes for the conformers are showed in Figs. 1–4.

3. Results and discussion

3.1. Glyphosate conformers, abundance

The Gibbs free energies were obtained from the frequency calculations, the entropy and thermal corrections. These energies were used to

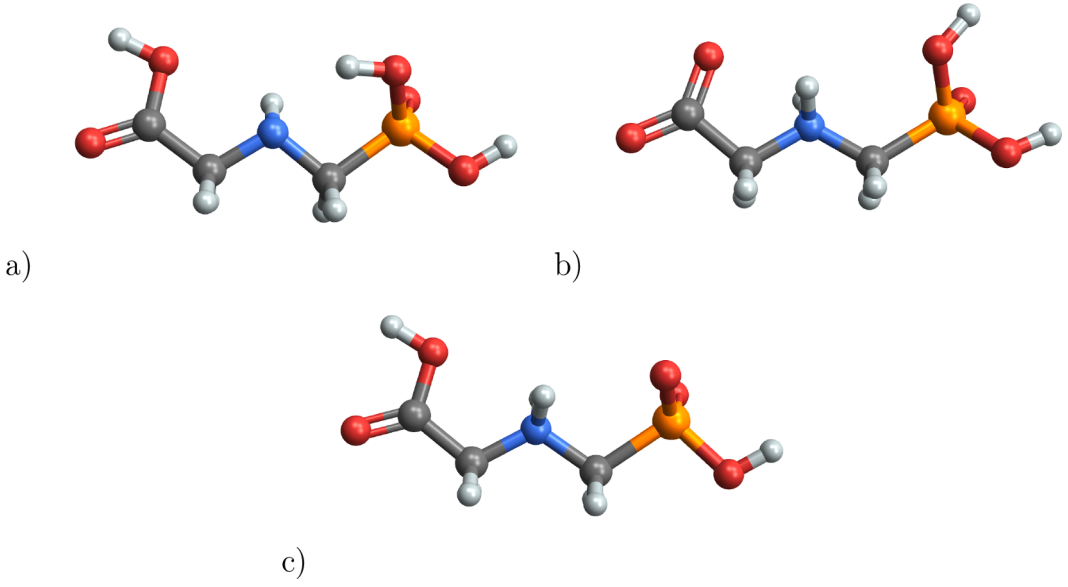

Fig. 1. Conformers for GLY a)4112 b)4202 c)4211.

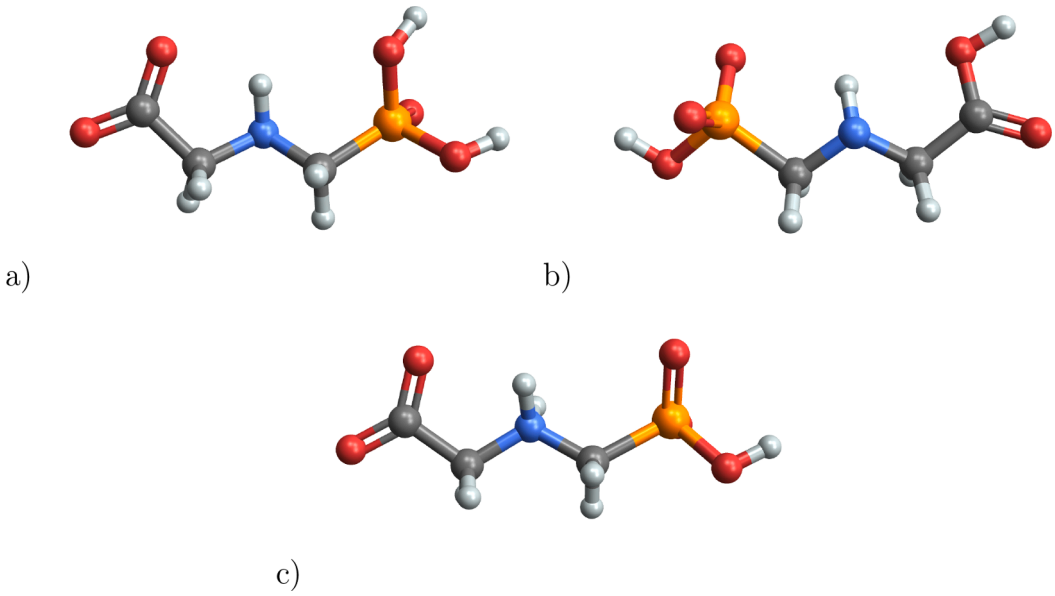

Fig. 2. Conformers for GLY^{-1} a)4102 b)4111 c)4201.

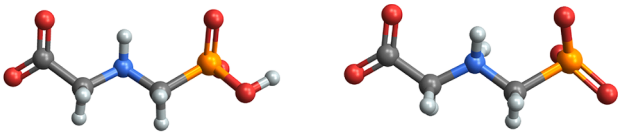

Fig. 3. Conformers for GLY^{-2} a)4101 b)4200 .

obtain the relative abundances of the glyphosate conformers, assuming that they have a Boltzmann distribution.

The Boltzmann populations of the isomers are computed through the probabilities defined in Eq. (1)

$$P_k(T) = \frac{e^{-\beta \Delta G_k}}{\sum_{i=1}^{n} e^{-\beta \Delta G_i}} \quad (1)$$

where β=1/k_BT, and k_B is the Boltzmann constant, T is the temperature in Kelvin, ΔG is the Gibbs free energy of the kth isomer. Eq. (1) establishes that the distribution of molecules will be among energy levels as a function of the energy and temperature. Eq. (1) is restricted so that the sum of all probabilities of occurrence, at fixed temperature T, Pi (T) is equal to 1 and given by Eq. (2)

$$\sum_{i=1}^{n} P_i = 1 \quad (2)$$

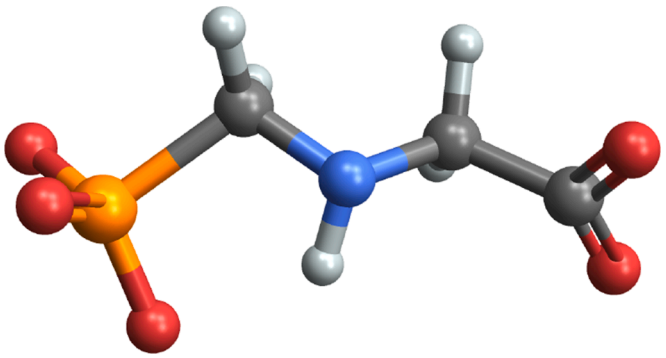

Fig. 4. Conformers for GLY^{-3} a)4100 .

The results are shown in Tables 3–5, Figs. 5–8.

Among the species with formal charge 0 (GLY), it is observed that there are clearly two types of conformers that are stable: those that are not ionized and the phosphonate zwitterions, while the population of carboxylate zwitterions is negligible. The relative amounts of both conformers in the different solvents vary with the level of theory used in the calculations and the different solvent models.

In the case of IEFPCM calculations, the non-ionized conformer is the most stable (4112) in all solvents except DMSO where zwitterion phosphonate (4211) is the most predominant. This last conformer can be observed in appreciable amounts in Acetone, Acetonitrile, DMSO, Ethanol and Water, that is, in solvents that have a certain degree of polarity.

When the formal charge is -1 (GLY^{-1}), the predominant species in almost all solvents is the 4201 conformer, that is, the species that has lost the hydrogen from the carboxylate group, except in the case of carbon tetrachloride, where the 4102 species is the one that dominates.

When the formal charge is -2 (GLY^{-2}) there is only the 4101 configuration and when the formal charge is -3 (GLY^{-3}), the 4100 specie.

As stated above, changing the solvent model changes the relative abundances of the different glyphosate configurations. In the SMD solvent model, when the formal charge is 0, it is observed that the 4112 species is the only species in most solvents, except for the case of Ethanol and water, where the predominant species is that of the zwitterion phosphonate, being almost the only species in the case of water. As in the IEFPCM model, the abundance of the zwitterion carboxylate is negligible. This is in agreement with previously found experimental results by XPS [28].

For formal charges -1, -2 and -3 the results using the SMD and IEFPCM models are the same. However, for the formal charge -2, the experimental results found by Pedano et al. [28] show that, in the case of water, the most favorable structure is 4200. This means that the use of the base 6-31G(d,p) it is not good at finding the minimum energy configuration. This is why we repeat the calculations using a larger basis (6-311++G(2d,2p)) and the SMD solvation model.

The results are displayed in the Table 3.

From the results for the case of water, it is observed that when the molecule has a neutral charge, the most stable form is the zwitterionic species with the protonated amino group and the phosphonate group with a deprotonation (species 4211), the first deprotonation occurs in

Table 3
Abundance of the conformers using IEFPCM solvation model and B3LYP/6-31G(d,p) level of theory.

Solvent	4112	4202	4211	4102	4111	4201	4101	4200	4100
CH_3COCH_3	78.2344	0.0154	21.7501	3.3e-05	-	100.0	99.9911	0.0089	100.0
CH_3CN	76.9637	0.0224	23.0138	3.1e-05	-	100.0	99.9892	0.0108	100.0
CH_2Cl_2	98.9042	0.0012	1.0946	5.6e-05	-	99.9999	99.9993	0.0007	100.0
CCl_4	99.9999	-	5.6e-05	100.0	-	1e-06	100.0	-	100.0
DMSO	32.7608	0.0163	67.2229	2.6e-05	-	100.0	99.9858	0.0142	100.0
EtOH	83.3411	0.0139	16.645	2.1e-05	-	100.0	99.9898	0.0102	100.0
H_2O	64.2655	0.0625	35.672	4.9e-05	-	100.0	99.9837	0.0163	100.0
Gas phase	100.0	-	-	0.0025	-	99.9975	100.0	-	100.0

Table 4
Abundance of the conformers using SMD solvation model and B3LYP/6-31G(d,p) level of theory.

Solvent	4112	4202	4211	4102	4111	4201	4101	4200	4100
CH_3COCH_3	99.9995	-	0.0005	0.0009	-	99.9991	100.0	2e-06	100.0
CH_3CN	99.9964	-	0.0036	0.0002	-	99.9998	100.0	2e-06	100.0
CH_2Cl_2	99.9668	-	0.0332	0.0002	-	99.9998	100.0	5e-06	100.0
CCl_4	100.0	-	1.1e-05	0.0013	-	99.9987	100.0	-	100.0
DMSO	99.992	-	0.008	0.0004	-	99.9996	100.0	1e-06	100.0
EtOH	37.6258	0.1284	62.2458	8e-06	-	100.0	99.8847	0.1153	100.0
H_2O	5.512	0.4179	94.0701	5e-06	-	100.0	99.002	0.998	100.0
Gas phase	100.0	-	-	0.0025	-	99.9975	100.0	-	100.0

the carboxylate group (forming species 4201), the second deprotonation at the phosphonate group (forming species 4200), and the last deprotonation at the amino group (forming species 4100).

All authors agree that the first deprotonated form of glyphosate is the 4201 species, however the second deprotonation of glyphosate has been the subject of controversy since authors such as Liu [35], using calorimetry and NMR techniques, and Peixoto [29], using DFT and the IEFPCM solvation model, found that this second deprotonation occurred in the amino group, giving rise to the formation of the 4101 species. While Ruano et al. [28], using XPS and DFT, and Yan et al. [36], using ATR-FTIR, Two-Dimensional Correlation Spectroscopy, and DFT Study, found that this second deprotonation occurs in the phosphonate group, as indicated by our study. It is important to highlight that although species 4200 is the predominant species in our study (58%), species 4101 cannot be neglected since it has a population close to 42%. This indicates that species 4101 and 4200 are in equilibrium and that experimentally it is possible to find evidence of the existence of both.

In the case of ethanol and acetonitrile, the zwitterionic species 4211 is also the most stable species when the formal charge is 0. However, in the case of acetonitrile, the 4112 species is also present in the majority.

Table 5
Abundance of the conformers using SMD solvation model and B3LYP/6-311++G(2d,2p) level of theory.

Solvent	4112	4202	4211	4102	4111	4201	4101	4200	4100
CH_3COCH_3	94.7471	0.6159	4.637	6e-06	-	100.0	100.0	4.9e-05	100.0
CH_3CN	38.6568	-	61.3432	1.1e-05	-	100.0	99.9998	0.0002	100.0
CH_2Cl_2	98.4792	0.3416	1.1792	9e-06	-	100.0	99.9999	0.0001	100.0
CCl_4	100.0	-	-	6.5e-05	-	99.9999	100.0	-	100.0
DMSO	90.6111	0.3003	9.0886	5e-06	-	100.0	100.0	4.9e-05	100.0
EtOH	0.3746	0.9679	98.6576	-	-	100.0	75.8688	24.1312	100.0
H_2O	0.1797	0.3196	99.5008	2e-06	-	100.0	41.9632	58.0368	100.0
Gas Phase	100.0	-	-	0.0001	-	99.9999	100.0	-	100.0

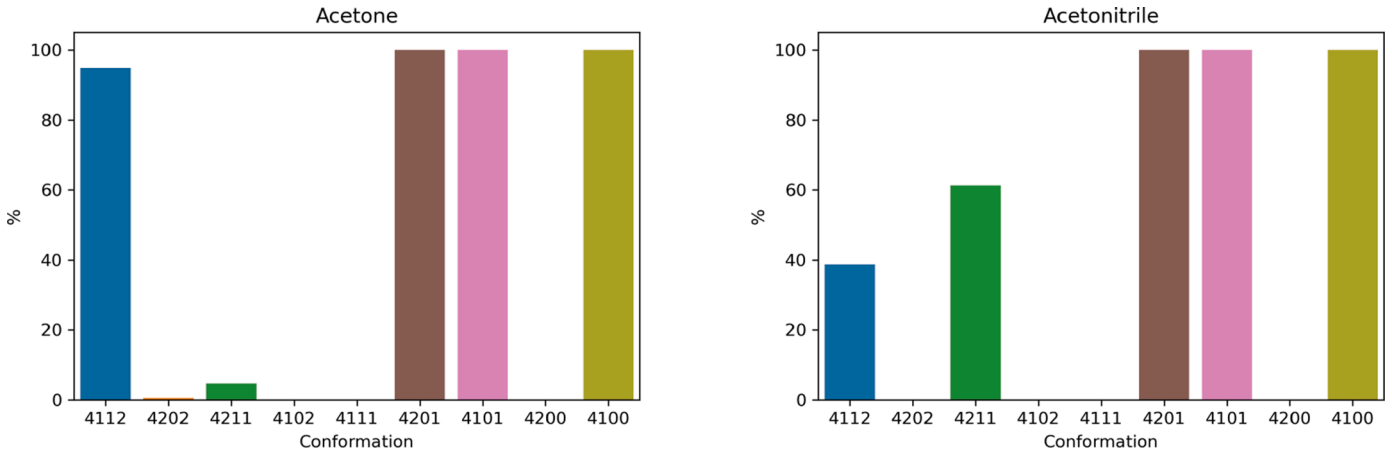

Fig. 5. Boltzmann population values for stable conformations found for different structures of glyphosate and its deprotonated forms in acetone and acetonitrile using SMD solvation model and B3LYP/6-311++G(2d,2p) level of theory.

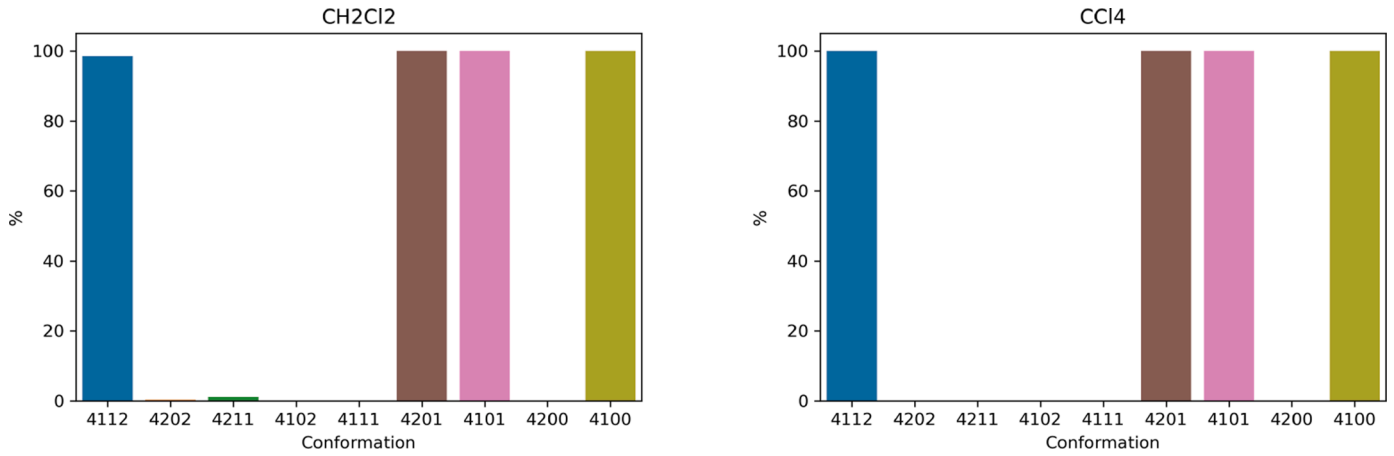

Fig. 6. Boltzmann population values for stable conformations found for different structures of glyphosate and its deprotonated forms in dichloromethane and tetrachloromethane using SMD solvation model and B3LYP/6-311++G(2d,2p) level of theory.

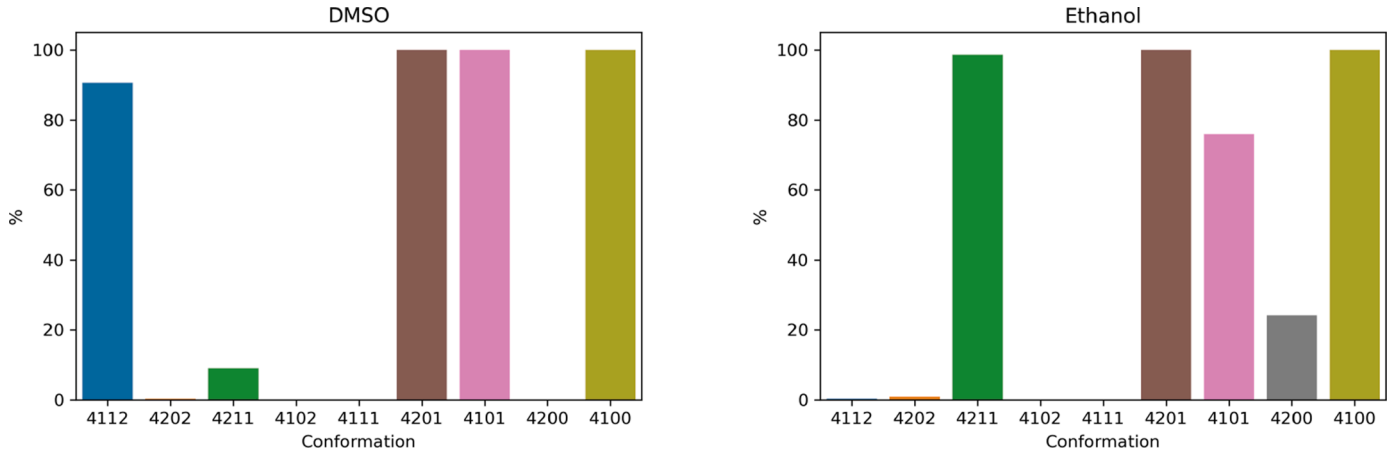

Fig. 7. Boltzmann population values for stable conformations found for different structures of glyphosate and its deprotonated forms in dimethylsulfoxide and ethanol using SMD solvation model and B3LYP/6-311++G(2d,2p) level of theory.

As in all the previous cases, the only species with a stable -1 formal charge is the 4201 species. The second deprotonation occurs, unlike in the case of water, in the phosphonate group, although in the case of ethanol the deprotonation can also be observed in the existence of the 4200 species, but in a smaller proportion than in the case of water.

In the rest of the solvents, the most stable species is the 4112 species when the formal charge is 0, then the 4201 species, and the second deprotonation occurs at the phosphonate group to form the 4101 species and finally the 4100 species. The results show that the solvent exerts a great influence with respect to the stability of the species in question. Protic solvents, such as water and ethanol, are the only ones capable of stabilizing the 4200 species in solution and for the 4211 species the

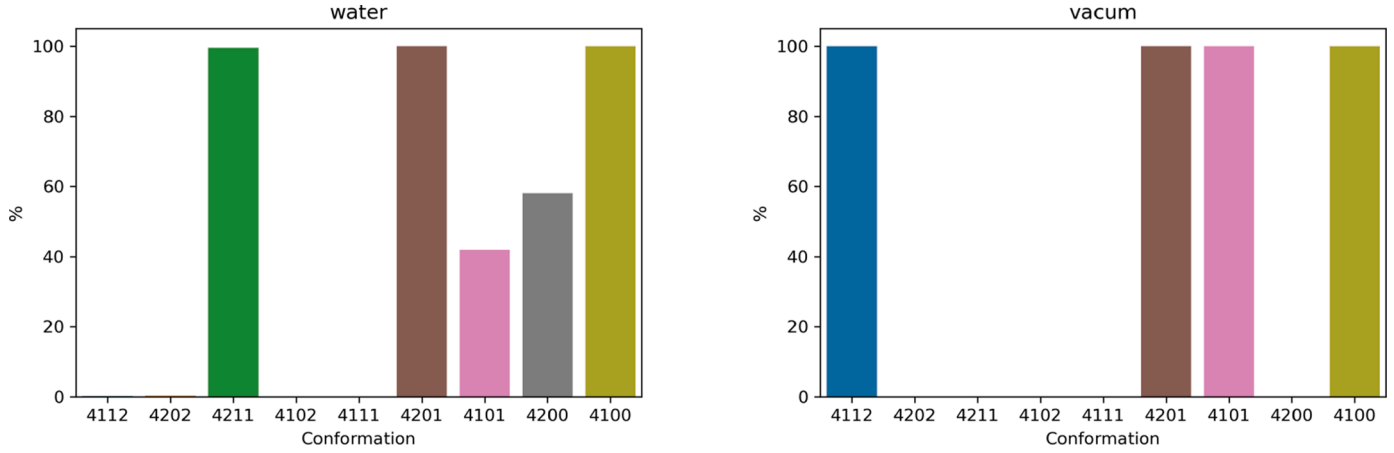

Fig. 8. Boltzmann population values for stable conformations found for different structures of glyphosate and its deprotonated forms in water and gas phase using SMD solvation model and B3LYP/6-311++G(2d,2p) level of theory.

Table 6
Theoretical vs experimental IR vibrational frequencies in cm^{-1} for GLY (4112).

Assigment	Expt[a]	gas phase	CH_3COCH_3	CH_3CN	CH_2Cl_2	CCl_4	DMSO	EtOH	H_2O
ν(N-H)	3243	3537	3552	3563	3531	3546	3552	3525	3552
ν(C═ O)	1732	1803	1775	1763	1770	1792	1778	1728	1701
δ(N-H)	1570	1518	1501	1498	1509	1509	1504	1507	1493
ν(P═ O)	1222	1269	1250	1238	1243	1261	1242	1213	1198

a)solid

Table 7
Theoretical vs experimental IR vibrational frequencies in cm^{-1} for GLY (4211).

Assignment	Expt[a]	H_2O	CH_3COCH_3	CH_3CN	CH_2Cl_2	DMSO	EtOH
ν(C═ O)	1740	1728	1786	1783	1795	1790	1882
δ(NH2)	1610	1532	1590	1605	1604	1659	1567
ν(C-OH)	1433	1436	1451	1464	1463	1479	1452
τ(NH2)	1384	1376	1255	1272	1211	1258	1370
ν(C-OH)/γ(C-O-H)	1244	1143	1176	1168	1186	1177	1298
ν_{as}(PO2)	1188	1204	1244	1242	1243	1247	1178
ν_s(PO2)	1076	1043	1070	1068	1066	1050	1063
ν(P-OH)	916	770	758	759	759	756	811

a)in water

Table 8
Theoretical vs experimental IR vibrational frequencies in cm^{-1} for GLY^{-1} (4201).

Assignment	Expt[a]	H_2O	CH_3COCH_3	CH_3CN	CH_2Cl_2	CCl_4	DMSO	EtOH	gas phase
ν_{as}(COO)	1614	1556	1670	1657	1665	1701	1672	1606	1722
δ(NH2)	1580	1484	1627	1590	1627	1654	1643	1563	1631
ν_s(COO)	1400	1344	1362	1365	1364	1349	1366	1379	1330
τ(CH2)/τ(NH2)	1228	1216	1192	1197	1190	1184	1193	1236	1216
ν_{as}(PO2)	1186	1199	1240	1233	1239	1264	1243	1207	1271
ν_s(PO2)	1080	1061	1060	1064	1063	1064	1063	1061	1063
ν(P-OH)	917	799	763	762	765	754	764	734	753

a)in water

relative amounts depend on its polarity.

3.2. IR Spectra

There are two main regions in the infrared spectrum of glyphosate, one with bands from 800 cm^{-1} to 1300 cm^{-1} belonging to the phosphonate group and the second with bands from 1300 cm^{-1} to 1800 cm^{-1} belonging to the amino and carboxyl groups [37].

Tables 6 and 7 show the results of the spectra obtained for glyphosate when the formal charge is 0 for the solid state and when it is in solution, for the solid state we consider that the predominant species, based on the DFT calculations, is species 4112 and in solution the predominant species is species 4211.

One of the differences that can be observed is the displacement of the δ mode of the NH, although they are found at a close frequency, in the case of species 4112, experimentally it is found at a lower frequency than in the case of the species 4211.

In the regions belonging to the phosphonate group, a peak is observed around 1200 cm^{-1}, which in the case of species 4112 is close to the vibrational mode ν(P═ O) and in the species 4112 corresponds to the $\nu_{as}(PO_2)$ mode. In the zwitterionic species, the $\nu_s(PO_2)$ mode is also observed at 1076 cm^{-1}, while in the neutral species don't.

In general terms, it can be seen that the calculated frequencies are lower than the experimental ones. The main differences are in the ν(C-OH)/γ(C-O-H) and ν(P-OH) modes. This last mode is poorly described by the method used in this work. Jin et al. [36], using a smaller base and explicit water molecules around glyphosate, found a value much closer to the experimental one, which would indicate that, in some way, the solvent plays an important role when it comes to describe those modes.

The vibrational frequencies for species 4201 are shown in the Table 8. According to calculations this species is the only possible one for GLY^{-1}. Again, an excellent agreement with the experimental data is observed. The only major difference, again, is seen in the ν(P-OH) mode.

Another of the discrepancies that exists is to know which are the species that exist for GLY^{-2}. It has already been mentioned that the two species are 4200 and 4101. It is interesting to see that both species can be differentiated by means of the IR spectrum (Table 9): both show the mode corresponding to ν_{as}(COO), but in the species 4200 is greater than in species 4101. The mode corresponding to ν_s(COO) is very similar in both cases, therefore, to see the differences between both species it is necessary to see which are the characteristic modes of each of them: in species 4101 the modes related to the movements of the hydrogens in the amino group are not found, that is, the modes $\delta(NH_2)$ and $\tau(NH_2)$. The modes ν(PO 3) are also not found. In the spectrum of species 4200, the ν_s(PO2) and ν_{as}(PO2) modes, as expected, are absent.

The spectrum of GLY^{-3} has only one possible interpretation. Table 10 shows the results of the calculations and their comparison with the experimental results. The correlation between them is excellent.

Table 9
Theoretical vs experimental IR vibrational frequencies in cm^{-1} for GLY^{-2} (4200).

Assignment	Expt[a]	H_2O	EtOH
ν_{as}(COO)	1610	1536	1576
δ(NH2)	1567	1598	1633
ν_s(COO)	1400	1383	1394
τ(NH2)	1372	1400	1409
ν(PO3) (E)	1094	1065	1070
ν(C-N)	1052	1039	1037
ν(PO3) (A1)	980	939	937

a) in water

Table 10
Theoretical vs experimental IR vibrational frequencies in cm^{-1} for GLY^{-2} (4101).

Assignment	Expt[a]	H_2O	CH_3COCH_3	CH_3CN	CH_2Cl_2	CCl_4	DMSO	EtOH	gas phase
ν_{as}(COO)	1610	1501	1600	1595	1595	1622	1605	1537	1628
ν_s(COO)	1400	1400	1385	1386	1386	1379	1385	1399	1364
ν(C-N)	1052	1087	1086	1086	1086	1075	1089	1082	1066
ν_{as}(PO2)	-	1169	1215	1209	1210	1222	1215	1177	1227
ν_s(PO2)	-	1045	1053	1050	1055	1047	1054	1046	1050

a)in water

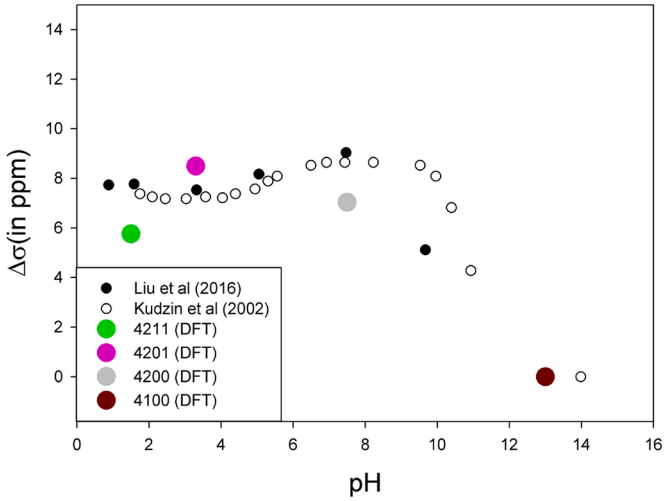

Fig. 9. pH dependence of ^{31}P NMR phosphorus shifts.

3.3. NMR

NMR spectroscopy is a powerful technique for studying both qualitative and quantitative relationships between different organic molecules.

In a recent work, Liu et al. [35], using this technique, determined the 31P NMR spectrum of glyphosate at different pHs: 13,7.5,3.4 and 1.0. The dominant species are assumed to be: GLY^{-3} (100%); solution b, GLY^{-2} (99%); solution c, GLY^{-1} (97%); and solution d, GLY (82%).

They found a shift between solution a) and solution b) of 8.83 ppm, and attributed this to the protonation of oxygen in the phosphonate group. For the second protonation the change is 1.48 ppm and they assume that it occurs at the amino group. The third protonation has a shift of -0.18 ppm. They justify these changes by taking into account the distance between the atom that is protonated and the phosphorus atom. That is, they assume that protonation has the following form: a)4100 101 201 211

Our calculations show that if this were the case, the displacements would be: 2.89 ppm, 11.38 ppm, and -2.73 ppm, respectively.

Instead, if we consider protonation to be of the form (as the Boltzmann population-based abundance results and IR spectra results show): b)4100 200 201 211

The displacement of the NMR signal would be: 7.02 ppm, 1.46 ppm and -2.73 ppm, the observed change is very similar to that obtained experimentally (Fig. 9).

Table 11 shows all the displacements obtained by DFT for the different solvents using H_3PO_4 as reference.

3.4. Conclusions

In the present work we have performed DFT calculations on glyphosate and its deprotonated forms using two implicit solvent models. The results show that the IEFPCM model is not a good model since it indicates that the neutral species (4112) is the most stable in aqueous solution, while the experimental results show that the most stable species is the zwitterionic (4211) when the charge formal is 0. On the contrary, the SMD method is capable of providing a correct description of the most stable form in aqueous solution. However, we also found that the size of the base set is also relevant when predicting the stability of a species: the use of a median base (6-31G(d,p)) shows that for the species with two negative charges is 4101, while using a larger basis (6-311++G (2d,2p)) shows that the more stable structure is 4200.

Taking this basis into account, we have been able to assign the vibrational modes found experimentally in aqueous solution and we have extended the assignment of the modes to the different solvents used in this study. Likewise, we have calculated the 31P NMR spectrum and have compared the results with experimental data and have reached the conclusion that the shift observed in the first protonation of glyphosate corresponds to the protonation on the amino group and not on the phosphonate group, as some authors claim.

We have extended the study to several solvents, with different

Table 11
Theoretical ^{31}P isotropic chemical shift for glyphosate species in different solvents.

	4112	4202	4211	4201	4101	4200	4100
CH_3COCH_3	26.84	12.48	3.41	3.94	11.58		11.73
CH_3CN	26.93		3.885	4.487	12.068		10.33
CH_2Cl_2	23.905	11.628	3.29	2.465	11.78		10.188
CCl_4	24.399		–4.145	3.152	10.704		10.993
DMSO	26.907	12.917	3.38	2.846	11.298		9.815
EtOH	24.457		0.145	2.155	13.378	4.305	10.94
H_2O	25.342	11.366	4.904	2.171	13.556	3.632	10.66
Gas Phase	21.2			1.787	9.529		13.078

polarities, in the hope that once the most stable glyphosate species are determined, this knowledge can help in the study of their characterization and better simulation in different environments.

Credit author statement

The authors contributed equally

Declaration of Competing Interest

The authors certify that they have NO affiliations with or involvement in any organization or entity with any financial interest (such as honoraria; educational grants; participation in speakers' bureaus; membership, employment, consultancies, stock ownership, or other equity interest; and expert testimony or patent-licensing arrangements), or non-fi nancial interest (such as personal or professional relationships, affiliations, knowledge or beliefs) in the subject matter or materials discussed in this manuscript.

Data availability

Data will be made available on request.

Acknowledgement

The authors thank CONICET and the ANPCyT (PICT-2019-4310)., Argentina. MEFH is a CONICET fellow

References

[1] G. Pasquarell, D. Boyer, Herbicides in Karst Groundwater in Southeast West Virginia. Technical Report, Wiley Online Library, 1996.
[2] E. Funari, L. Donati, D. Sandroni, M. Vighi, Pesticide levels in groundwater: value and limitations of monitoring. Pesticide Risk in Groundwater, CRC Press, 2019, pp. 3–44.
[3] W. Skeff, C. Recknagel, D.E. Schulz-Bull, The influence of salt matrices on the reversed-phase liquid chromatography behavior and electrospray ionization tandem mass spectrometry detection of glyphosate, glufosinate, aminomethylphosphonic acid and 2-aminoethylphosphonic acid in water, J. Chromatogr. A 1475 (2016) 64–73.
[4] L. Sun, D. Kong, W. Gu, X. Guo, W. Tao, Z. Shan, Y. Wang, N. Wang, Determination of glyphosate in soil/sludge by high performance liquid chromatography, J. Chromatogr. A 1502 (2017) 8–13.
[5] F. Fang, R. Wei, X. Liu, S. Li, et al., Determination of glyphosate by HPLC with a novel pre-column derivatization reagent, Chin. J. Bioprocess Eng. 12 (3) (2014) 69–72.
[6] J. Ding, H. Guo, W.-w. Liu, W.-w. Zhang, J.-w. Wang, Current progress on the detection of glyphosate in environmental samples, J. Sci. Appl. Biomed. 3 (06) (2015) 88–95.
[7] M. Ibáñez, Ó.J. Pozo, J.V. Sancho, F.J. López, F. Hernández, Residue determination of glyphosate, glufosinate and aminomethylphosphonic acid in water and soil samples by liquid chromatography coupled to electrospray tandem mass spectrometry, J. Chromatogr. A 1081 (2) (2005) 145–155.
[8] Y. Liao, J.-M. Berthion, I. Colet, M. Merlo, A. Nougadère, R. Hu, Validation and application of analytical method for glyphosate and glufosinate in foods by liquid chromatography-tandem mass spectrometry, J. Chromatogr. A 1549 (2018) 31–38.
[9] D. Wang, B. Lin, Y. Cao, M. Guo, Y. Yu, A highly selective and sensitive fluorescence detection method of glyphosate based on an immune reaction strategy of carbon dot labeled antibody and antigen magnetic beads, J. Agric. Food Chem. 64 (30) (2016) 6042–6050.
[10] A.S. da Silva, F.C.B. Fernandes, J.O. Tognolli, L. Pezza, H.R. Pezza, A simple and green analytical method for determination of glyphosate in commercial formulations and water by diffuse reflectance spectroscopy, Spectrochim. Acta, Part A 79 (5) (2011) 1881–1885.
[11] H. Torul, İ.H. Boyaci, U. Tamer, Attomole detection of glyphosate by surface-enhanced raman spectroscopy using gold nanorods, FABAD J. Pharm. Sci 35 (2010) 179–184.
[12] X. Ding, K.-L. Yang, Development of an oligopeptide functionalized surface plasmon resonance biosensor for online detection of glyphosate, Anal. Chem. 85 (12) (2013) 5727–5733.
[13] B. Cartigny, N. Azaroual, M. Imbenotte, D. Mathieu, G. Vermeersch, J. Goullé, M. Lhermitte, Determination of glyphosate in biological fluids by 1h and 31p nmr spectroscopy, Forensic Sci. Int. 143 (2–3) (2004) 141–145.
[14] E.A. Songa, T. Waryo, N. Jahed, P.G. Baker, B.V. Kgarebe, E.I. Iwuoha, Electrochemical nanobiosensor for glyphosate herbicide and its metabolite, Electroanal. Int. J. Devoted Fundam. Pract. Asp. Electroanal. 21 (3–5) (2009) 671–674.
[15] B.B. Prasad, D. Jauhari, M.P. Tiwari, Doubly imprinted polymer nanofilm-modified electrochemical sensor for ultra-trace simultaneous analysis of glyphosate and glufosinate, Biosens. Bioelectron. 59 (2014) 81–88.
[16] H.H. See, P.C. Hauser, W.A.W. Ibrahim, M.M. Sanagi, Rapid and direct determination of glyphosate, glufosinate, and aminophosphonic acid by online preconcentration ce with contactless conductivity detection, Electrophoresis 31 (3) (2010) 575–582.
[17] Z. Liu, M. Zhu, P. Yu, Y. Xu, X. Zhao, Pretreatment of membrane separation of glyphosate mother liquor using a precipitation method, Desalination 313 (2013) 140–144.
[18] H. Lan, W. He, A. Wang, R. Liu, H. Liu, J. Qu, C. Huang, An activated carbon fiber cathode for the degradation of glyphosate in aqueous solutions by the electro-fenton mode: optimal operational conditions and the deposition of iron on cathode on electrode reusability, Water Res. 105 (2016) 575–582.
[19] B. Xing, H. Chen, X. Zhang, Efficient degradation of organic phosphorus in glyphosate wastewater by catalytic wet oxidation using modified activated carbon as a catalyst, Environ. Technol. 39 (6) (2018) 749–758.
[20] L. Loperena, M.D. Ferrari, V. Saravia, D. Murro, C. Lima, A. Fernández, C. Lareo, et al., Performance of a commercial inoculum for the aerobic biodegradation of a high fat content dairy wastewater, Bioresour. Technol. 98 (5) (2007) 1045–1051.
[21] C. Zhou, D. Jia, M. Liu, X. Liu, C. Li, Removal of glyphosate from aqueous solution using nanosized copper hydroxide modified resin: equilibrium isotherms and kinetics, J. Chem. Eng. Data 62 (10) (2017) 3585–3592.
[22] T.R. Santos, M.B. Andrade, M.F. Silva, R. Bergamasco, S. Hamoudi, Development of α-and γ-fe2o3 decorated graphene oxides for glyphosate removal from water, Environ Technol 40 (9) (2019) 1118–1137.
[23] L. Guo, Y. Cao, K. Jin, L. Han, G. Li, J. Liu, S. Ma, Adsorption characteristics of glyphosate on cross-linked amino-starch, J. Chem. Eng. Data 63 (2) (2018) 422–428.
[24] S. Zavareh, Z. Farrokhzad, F. Darvishi, Modification of zeolite 4a for use as an adsorbent for glyphosate and as an antibacterial agent for water, Ecotoxicol. Environ. Saf. 155 (2018) 1–8.
[25] N.A. Pérez-Chávez, A.G. Albesa, G.S. Longo, Molecular theory of glyphosate adsorption to pH-responsive polymer layers, Adsorption 25 (7) (2019) 1307–1316.
[26] N.A. Pérez-Chávez, A.G. Albesa, G.S. Longo, Using polymer hydrogels for glyphosate sequestration from aqueous solutions: molecular theory study of adsorption to polyallylamine films, Langmuir 34 (42) (2018) 12560–12568.
[27] O. Fliss, K. Essalah, A.B. Fredj, Stabilization of glyphosate zwitterions and conformational/tautomerism mechanism in aqueous solution: insights from ab initio and density functional theory-continuum model calculations, PCCP 23 (46) (2021) 26306–26323.
[28] G. Ruano, M. Pedano, M. Albornoz, J. Fuhr, M. Martiarena, G. Zampieri, Deprotonation of the amine group of glyphosate studied by xps and dft, Appl. Surf. Sci. 567 (2021) 150753.
[29] M.M. Peixoto, G.F. Bauerfeldt, M.H. Herbst, M.S. Pereira, C.O. da Silva, Study of the stepwise deprotonation reactions of glyphosate and the corresponding p k a values in aqueous solution, J. Phys. Chem. A 119 (21) (2015) 5241–5249.
[30] W. Kohn, L.J. Sham, Self-consistent equations including exchange and correlation effects, Phys. Rev. 140 (4A) (1965) A1133.
[31] R.G. Parr, Density functional theory of atoms and molecules. Horizons of Quantum Chemistry, Springer, 1980, pp. 5–15.
[32] F. Neese, The orca program system, Wiley Interdiscip. Rev. Comput. Mol. Sci. 2 (1) (2012) 73–78.
[33] E. Cances, B. Mennucci, J. Tomasi, A new integral equation formalism for the polarizable continuum model: theoretical background and applications to isotropic and anisotropic dielectrics, J. Chem. Phys. 107 (8) (1997) 3032–3041.
[34] A.V. Marenich, C.J. Cramer, D.G. Truhlar, Universal solvation model based on solute electron density and on a continuum model of the solvent defined by the bulk dielectric constant and atomic surface tensions, J. Phys. Chem. B 113 (18) (2009) 6378–6396.
[35] B. Liu, L. Dong, Q. Yu, X. Li, F. Wu, Z. Tan, S. Luo, Thermodynamic study on the protonation reactions of glyphosate in aqueous solution: potentiometry, calorimetry and NMR spectroscopy, J. Phys. Chem. B 120 (9) (2016) 2132–2137.
[36] W. Yan, C. Jing, Molecular insights into glyphosate adsorption to goethite gained from ATR-FTIR, two-dimensional correlation spectroscopy, and dft study, Environ. Sci. Technol. 52 (4) (2018) 1946–1953.
[37] R.C. Pereira, A.C. da Costa, F.F. Ivashita, A. Paesano Jr, D.A. Zaia, Interaction between glyphosate and montmorillonite in the presence of artificial seawater, Heliyon 6 (3) (2020) e03532.